


FULL ARTICLE

Investigation of the effect of clinically relevant interferents on glucose monitoring using near-infrared spectroscopy

Silje Skeide Fuglerud^{1,2*}  | Reinold Ellingsen¹ | Astrid Aksnes¹ |
Dag Roar Hjelme¹

¹Department of Electronic Systems, Norwegian University of Science and Technology, Trondheim, Norway

²Department of Endocrinology, St. Olavs University Hospital, Trondheim, Norway

*Correspondence

Silje Skeide Fuglerud, Department of Electronic Systems, Norwegian University of Science and Technology, O. S. Bragstads plass 2b, 7491 Trondheim, Norway.

Email: silje.fuglerud@ntnu.no

Funding information

Helse Midt-Norge, Grant/Award Number: 46055510; Norges Forskningsråd, Grant/Award Number: 248872

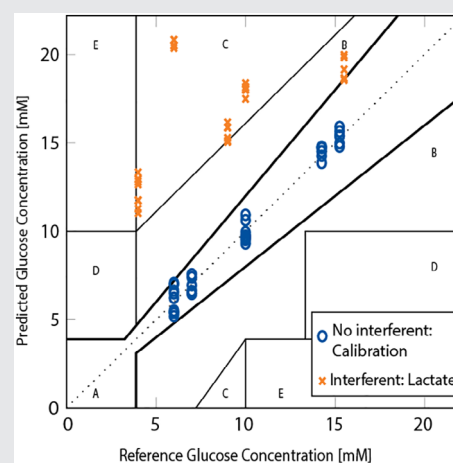
Abstract

Near infrared spectroscopy (NIR) is a promising technique for continuous blood glucose monitoring for diabetic patients. Four interferents, at physiological concentrations, were introduced to study how the glucose predictions varied with a standard multivariate calibration model. Lactate and ethanol were found to interfere strongly with the glucose predictions unless they were included in the calibration

models. Lactate was mistaken for glucose and gave erroneously high glucose predictions, with a dose response of 0.46 mM/mM. The presence of ethanol resulted in too low glucose predictions, with a dose response of -0.43 mM/mM. Acetaminophen, a known interferent in the glucose monitoring devices used for diabetes management today, was not found to be an interferent in NIR spectroscopy, nor was caffeine. Thus, interferents that may appear in high concentrations, such as ethanol and lactate, must be included in the calibration or model building of future NIR-based glucose measurement devices for diabetes monitoring.

KEYWORDS

acetaminophen, diabetes mellitus, ethanol, glucose, lactate, NIR, PLSR



Abbreviations: APAP, acetaminophen; CGM, continuous glucose monitoring; DM1, diabetes mellitus type 1; LV, latent variable; NIR, near-infrared; PLSR, partial least squares regression; rms, root mean square; RMSE, root mean square error; RMSECV, root mean square error of cross-validation; RMSEP, root mean square error of prediction; SNR, signal to noise ratio.

1 | INTRODUCTION

In pursuit of more effective treatment for diabetes mellitus type 1 (DM1), reliable glucose measurements are vital to achieve good blood glucose control (blood glucose

This is an open access article under the terms of the Creative Commons Attribution-NonCommercial License, which permits use, distribution and reproduction in any medium, provided the original work is properly cited and is not used for commercial purposes.

© 2021 The Authors. *Journal of Biophotonics* published by Wiley-VCH GmbH.

levels of 4–10 mM). The goal is to avoid harmful effects of either too high (hyperglycemia) or too low (hypoglycemia) blood sugar levels, of which the first can cause several long-term complications, including damages to the nervous system and vision, poorer general health and premature death. The current gold standard for glucose sensing is continuous subcutaneous measurements, where an electrochemical sensor is placed in the subcutaneous tissue just beneath the skin. There it measures glucose in the interstitial fluid surrounding the sensor. These sensors are selective to glucose and have clinically acceptable accuracy. However, the continuous glucose monitoring (CGM) sensors have a limited lifetime, suffer from interference from certain drugs [1, 2], and most need frequent calibrations. With the recent introduction of some pre-calibrated CGMs, the inconvenience of frequent calibrations is eliminated. As an alternative, optical glucose sensing could provide a long-term option for continuous glucose measurements.

Optical glucose sensing is not yet widely realized, but several options have been researched and there have been attempts of commercialization [3]. One method is near-infrared (NIR) spectroscopy (wavelengths 700–2500 nm), which is promising due to the availability of relatively low-cost optical components and sources, and because the penetration depth (0.5–4 mm) of the NIR wavelengths in human skin could enable non-invasive measurements [4–6]. However, the NIR bands are broad and relatively weak, which is related to challenges with low signal to noise ratios (SNRs). The accuracy of the predictions is therefore vulnerable to factors such as temperature variations, noise in the instrumentation, and uncalibrated changes in sample composition. Therefore, non-invasive NIR techniques face serious challenges due to inter-individual and time varying differences in tissue morphology and tissue components. Invasive NIR techniques, measuring directly in body fluids, represents a much simpler measurement problem and remains a promising glucose monitoring technique for future artificial pancreas based on glucose monitoring in for example the peritoneal cavity [7–9].

The success of NIR spectroscopy as a measurement method relies heavily on correct calibration and model building [10]. If the calibration model is applied to a sample containing molecules absorbing at the same wavelengths as glucose which were not present when calibrating and building the model, these molecules (interferents) may interfere with the accuracy of the glucose prediction.

Several studies exist on how to diminish effects of interferents in NIR spectra by data processing [11–13], or how to predict the concentration of several molecules simultaneously [14–22]. However, such correction methods often require a priori information about e.g. possible interferents not included in the calibration. To

achieve this, the interferents must be known. Some studies have investigated the effect of other sugars or glycated hemoglobin as interferents [11, 12, 23, 24] for glucose sensing, but several other potential interferents are left unexplored. Calibration of multivariate models for clinical use is particularly challenging. First, such calibration model building might require knowledge of the actual concentrations of the interferents, which may not be feasible unless the patients are in clinics. Second, the model calibration would require sufficient variation in interferent concentrations, something that would require monitoring over extensive time intervals, or worse, never occur. Thus, it is of great interest to quantify the glucose prediction errors resulting from unaccounted interferents.

In this study, we aim at exploring how the predictive ability of a glucose model is affected by the presence of four clinically relevant possible interferents; lactate, ethanol, acetaminophen (APAP) and caffeine. The ultimate goal is to contribute to the transformation from *in vitro* to *in vivo* NIR glucose measurements with high confidence. The model is based on non-biological samples, but the results should be transferable to the measurement in water-dominant bodily fluids. To verify this, a smaller study was conducted with intraperitoneal fluid spiked with one of the interferents. Lactate was chosen because it has a spectrum relatively similar to glucose and occurs naturally in the body.

Lactate is usually found at lower concentrations than glucose, but can in certain situations be comparable. During a workout, lactate is formed from the blood glucose when insufficient oxygen is available for complete oxidation of glucose to CO_2 and H_2O [25]. Lactate levels can also rise during infections such as the common cold or the flu, when glucose levels in patients with DM1 also tend to become elevated. Providing an accurate glucose measurement is essential in such circumstances. Lactate is one of the molecules that has been predicted simultaneously with glucose in some studies [15, 19, 21, 22], but to our knowledge the effect of leaving out lactate in the calibration model has not yet been examined. In physiological samples that could form the basis for a calibration model, one would not expect the lactate levels to be high unless specifically planned for. In this study, we therefore aimed to investigate how a glucose prediction model might behave with soaring lactate levels if the calibration did not include high lactate concentrations.

Ethanol was chosen because it is a popular substance that affects blood glucose levels [26, 27] and can be found in comparable concentrations to glucose in the blood. When a patient with DM1 is under the influence of alcohol, the glucose metabolism is affected and the judgment is impaired. From a clinical point of view, erroneous glucose measurements could be more serious (lead to hyper- or hypoglycemia).

Caffeine was chosen because the absorption spectrum exhibits similar absorption peaks as glucose in the combination band (2000-2500 nm), and it is a commonly ingested substance that can have an effect on the glucose levels of diabetes patients [28]. Caffeine is sometimes consumed in high-sugar beverages (coffee with milk, energy drinks), where the blood glucose levels tend to soar. If caffeine were to interfere with the glucose prediction it would therefore be a useful discovery.

APAP was chosen because it is a known interferent with the current enzymatic CGM devices [29], which certain manufacturers are working to solve [30]. APAP is present in drugs such as paracetamol that can be bought prescription free in many countries, and is used frequently for self-medication for numerous ailments. It is perhaps less well known that APAP also is an interferent for the glucose meters [1]. If APAP is not an interferent when measuring with NIR spectroscopy, it would be an advantage over the current gold standard.

Since APAP and caffeine are found at low concentrations in the body compared to glucose, lactate and ethanol, they were not expected to have a large impact on the absorption signal.

2 | EXPERIMENTAL

2.1 | Samples

Glucose in the range 0 to 50 mM was mixed with four interferents: lactate (0-30 mM), ethanol (0-69 mM), caffeine (0-0.05 mM), and APAP (0-0.3 mM), in phosphate buffered saline (tablets from VWR Life Science, PA, USA, 10 mM, pH 7) for stable pH. The analytes were obtained in powder form from Sigma Aldrich (MO, USA). The analyte concentrations were chosen to span physiological ranges with more extreme high end-points. Many other studies of optical glucose sensing have a slightly narrower glucose range, up to around 30 mM, but some also look at ranges similar or wider to what has been investigated here [3]. The lactate concentrations are similar to some studies determining lactate and glucose simultaneously [19, 21]. In a previous investigative study of APAP for amperometric devices, up to 26 mg/L (corresponding to 0.43 mM) was measured [30].

The sample mixtures were designed using Design Expert (Stat-Ease, MN, US) and an I-optimal model was chosen [31] covering the full sample space with 42 calibration samples. There were no significant correlations between the concentrations of glucose and the interferents. These samples were replicated in three chemically independent batches. In addition, a validation set of 42 samples was prepared, spanning the same sample space but with different concentrations.

2.2 | NIR measurements

The study was conducted at Nofima AS (Norway) using a NIR Systems XDS Rapid Content Analyzer Spectrometer (Metrohm Nordic AS, Norway) equipped with silicon (Si) and lead sulfide (PbS) detectors, covering the visible and short wave NIR (400-1100 nm) and NIR wavelengths (1100-2500 nm), respectively. Three quartz cuvettes of 1 mm path length were used. The cuvettes were placed in a cuvette holder which automatically pulled and centered the cuvette inside the spectrometer where it was illuminated by a broadband beam from a 50 W lamp. The beam path was not accessible or changed in the course of the experiment. The output of the spectrometer was the sample absorbance: $A = -\log(I/I_0)$ with arbitrary units (AU). The cuvette was placed in a heating block that was set to 37°C. However, there was no mechanism to cool down the sample which was heated by the beam while being scanned.

The 42×3 calibration spectra were collected in triplicate in the wavelength range 400 to 2500 nm sampling every 0.5 nm (4200 wavelength channels) with a bandwidth of 8.75 nm in the course of 4 days, giving a total of 359 spectra after some measurements were lost due to technical errors. On the fifth day, the validation set was collected, giving a dataset with 120 spectra.

Spectra of 100 mM of the interferents and glucose are shown in Figure 1.

2.3 | Chemometric analysis

Due to the many wavelength channels and relation in absorption between them, NIR spectroscopy models are often built using multivariate regression (chemometrics). Partial least squares regression (PLSR) is such a method employed to build a linear model from a calibration set [22, 32].

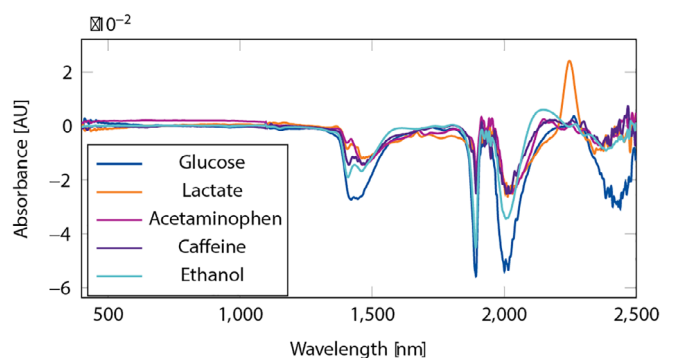


FIGURE 1 Spectral deviation of 100 mM spectra of interferents in phosphate buffered saline. The mean water spectrum was subtracted for visibility, as the water absorption is dominating

In short, PLSR performs a dimensionality reduction of the calibration spectra \mathbf{X} and the glucose values, \mathbf{Y} into latent variables (LVs) which maximally capture the covariance between \mathbf{X} and \mathbf{Y} . The vector of regression coefficients \mathbf{b} is a combination of the first few LVs. The number of LVs are determined based on the minimum root mean square error (RMSE) of the model applied to either subsets of the calibration measurements that were kept out of the model building (cross-validation), or a measurement set completely detached from the calibration measurements. Including too many LVs can lead to over-fitting and less robust models, it is therefore an important step in the model building.

A plethora of preprocessing methods exist, for spectral smoothing, removing spectral noise (for example from scattering and path length changes), or choosing spectral ranges with the most information. The choice of preprocessing was found using in-house code publicly available [33], iterating through derivatives, smoothing and scattering correction options. The success of the preprocessing was evaluated based on root mean square error of cross-validation (RMSECV) of a PLSR model. The most reliable and robust models were found when the only preprocessing applied was downweighting of certain noisy wavelengths. The downweighted regions were: highly absorbing water peaks (1800-2100 nm, 2300-2500 nm), the overlap of the two spectrometer detectors (1090-1110 nm), and the fringes of the detectors (<500 and >2300 nm), leaving 2956 wavelength channels unweighted. A selection of the most informative wavelength channels is not uncommon [20, 34], here we removed wavelengths that had low SNR either due to the detectors or almost all light being absorbed by the water and did not attempt to select regions with more or less glucose features. An example of a spectrum with downweighted regions is shown in Figure 2, where the spectral shape is determined by water.

The sample handling and cuvette cleaning was improved in the course of the experiment, including better

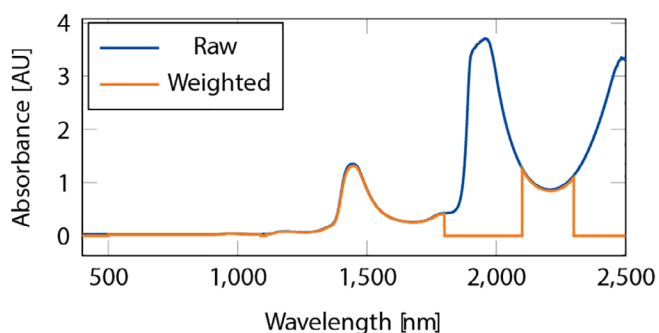


FIGURE 2 Example of one of the sample spectra with the downweighted regions. Water absorption dominates

handling to reduce temperature variations. The first 86 samples did not benefit from this improvement, and displayed a larger variability and prediction error. They were removed from the rest of the analysis on the basis of non-optimal sample handling. The rest of the sample set with 273 spectra was analyzed in full with a PLSR in Matlab (Statistics and Machine Learning Toolbox, Release 2020a, The MathWorks, Inc., MA, USA, *plsregress*) and a leave 10 out cross-validation which ensured that the duplicates were binned together. The validation set was held separate from the choice of parameters and the finished model was applied at the end of the analysis.

The sample set was then divided into five subsets: four subsets where one of the interferences was kept at zero, with 59 to 73 samples in each subset and the average of 10 random subsets (keeping duplicate measurements together). The 10 random subsets were generated to have a reliable comparison with the smaller sets that have one of the interferences left out. The random subsets had 45 to 78 included samples. New models were generated based on these subsets, and trained with cross-validation with batches of 15. The number of LVs was chosen based on the RMSECV to obtain the best possible model. That is, the models were built without any knowledge of the left-out interferent in question. The model was then applied to the rest of the sample set, which varied for each subset (labeled interferences in Table 1). At the end of the procedure, the model was applied to the validation set, which was unchanged for all subsets and is therefore the basis of comparison. In the presence of an interferent, a systematic increase in error should be seen with increasing interferent concentration. To investigate this, the average error was plotted as a function of interferent concentration, and in the case of a significant increase in error, the dose response was found by linear regression (*regress*, Matlab).

2.4 | Verification using biological samples

The limited verification study on biological samples was performed using a lensed fiber-based transmission spectroscopy setup with a broadband light source (SLS201L, Thorlabs, NJ, USA) and a NIRQuest512-2.5 spectrometer (Ocean Optics, FL, USA) [35]. Standard multi-mode fibers (0.22 NA M15L01, Thorlabs) were lensed using an FSM-100P ARC- Master (Fujikura, Japan) and were fixed with two fiber chucks (Newport, CA, USA) and aligned approximately 0.64 mm apart.

Porcine samples of intraperitoneal fluid was collected from two pigs during unpublished pilot experiments (date: 6 June 2019 and 11 June 2019, kept frozen) performed similarly to other work from our group [36, 37].

TABLE 1 The RMSEP for the models created based on the different sets

Model number	LVs	RMSEP interferences	RMSEP validation
1. Full	11	—	1.6 mM
2. Random sub (avg.)	9–11	3.1 mM	2.2 mM
3. No lactate	8	10.4 mM	6.3 mM
4. No ethanol	9	20.4 mM	17.9 mM
5. No APAP	9	3.6 mM	2.7 mM
6. No caffeine	9	3.4 mM	2.7 mM

Note: The RMSEP for interferences refers to the error of the model created by the subset applied to the rest of the full calibration set used in model 1. This is then the RMSEP from the set containing the interference that was not included in model 3–6.

Abbreviations: APAP, acetaminophen; RMSEP, root mean square error of prediction.

The intraperitoneal fluid samples were spiked with glucose and lactate in powder form to avoid diluting the fluid. Due to a limited amount of biological sample, this put some constraints on the number of samples measured, and limited the number of low concentrations. The sample was spiked further with glucose and/or lactate, yielding a total of 38 mixtures measured, where 18 samples were without lactate. Supra-physiological concentrations were included to increase the number of samples and to ensure that the limit of detection was exceeded, as the experimental setup has higher noise levels than the spectrometer used in the main study.

A volume of 100 μ L of the sample was applied as a droplet and measured on the lensed fibers immediately after mixing in the glucose or lactate powder. The transmission setup was cleaned with ethanol and water between every sample measurement. A spectrum of air and water was taken before every sample measurement. The transmission spectra were acquired using an integration time of 10 ms and 500 averages, followed by averaging over three spectra. The spectra were subjected to Savitzky–Golay smoothing (11 point smoothing, second order) prior to further analysis.

The absorbance spectra were found from the collected spectra by Beer–Lambert’s law, where I_0 referred to the air measurement. The water spectrum taken just before the sample was subtracted before analysis. These spectra were analyzed in the same way as the full data set, but only had one subset of 18 samples that did not contain lactate. The cross-validation was performed with leaving 25% of the samples out due to the small number of samples of the subset.

3 | RESULTS AND DISCUSSION

3.1 | Model performance

The root mean square error of prediction (RMSEP) of the models are shown in Table 1. Model 1 gave a prediction on the validation set with an RMSEP of 1.6 mM. The

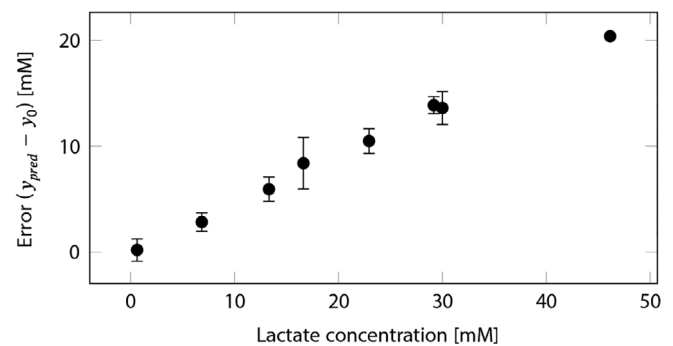


FIGURE 3 The absolute error ($y_{pred} - y_0$) of glucose model number 3 generated without lactate applied to the rest of the sample set (containing lactate) and the validation set, as a function of lactate concentration. The error points are grouped in bins in intervals of 5 mM for easier readability

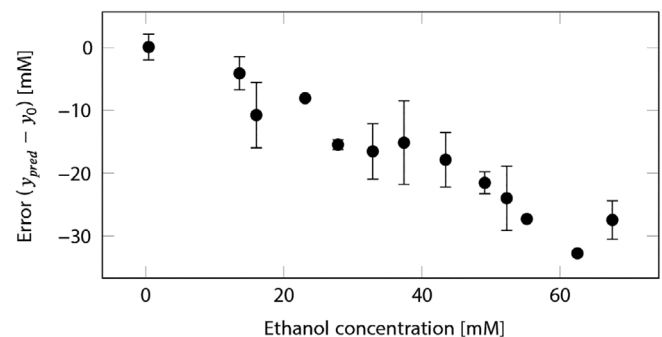


FIGURE 4 The absolute error ($y_{pred} - y_0$) of glucose model number 4 generated without ethanol applied to the rest of the sample set (containing ethanol) and the validation set, as a function of ethanol concentration. The error points are grouped in bins in intervals of 5 mM for easier readability

average error is shown for the 10 random subsets (labeled model 2). The RMSEP of validation varied from 1.0 to 3.8 mM. We can therefore assume that models 5 and 6 built from the subset without APAP and caffeine perform within the limit of random fluctuations. Models 3 and 4 built with an absence of lactate and ethanol performed worse.

We investigate model number 3 (built without lactate) and 4 (built without ethanol) further. Figure 3 shows a plot of the difference in the predicted glucose concentrations from the real glucose concentration from model number 3 as a function of the lactate concentration. The model performed poorly for high lactate concentrations. The dose response for glucose is an elevation in prediction of 0.46 mM per mM lactate (95% confidence interval [0.45, 0.47] mM). The model treats lactate as glucose, and an increase in lactate is wrongly assigned to an increase in glucose. This is also seen clearly in the Clarke Error Grid plot in Figure 6. Figure 4 shows a plot of the error of the glucose estimate of model number 4 as a function of the ethanol concentration. The model performed worse for increasing ethanol concentrations. Higher ethanol concentrations wrongfully decreased the glucose prediction, meaning that the ethanol obfuscates the glucose absorption, or absorb at wavelengths that model number 4 has assigned to negatively correlate with the presence of glucose. The dose response on the glucose prediction is approximately a decrease of -0.43 mM per mM ethanol (95% confidence interval $[-0.44, 0.42]$ mM).

3.2 | Clinical significance

A way to evaluate the clinical accuracy of a new glucose measurement device for diabetes treatment is through the Clarke Error Grid [38]. The results of the analysis on the full set is plotted in such an error grid in Figure 5, where measurement results that fall in zones A and B will lead to correct treatment (insulin being administered with high blood glucose values, no insulin injections for

low glucose values). Measurements in zones C and D will give information that will lead to unnecessary or lack of necessary treatment, and predictions in zone E would indicate that the patient is hypoglycemic when in reality hyperglycemic and vice versa [3]. A sensor should preferably only have predictions in zone A. Some predictions in zone B are also deemed acceptable, but there should never be predictions in zone E. The results on the validation set are compared directly. A summary of the results is presented in Table 2. The performance of the full model is adequate with most predictions in Zone A and only two predictions in zone B. The average of the 10 random subsets are given. The percentage of points in zone A ranged from 61.7% to 100%, with a median of 88.9%.

The models built without lactate and ethanol stand out as giving particularly poor results. The Clarke Error Grid is plotted for model number 3 without lactate in Figure 6. The presence of lactate places many of the predictions in zone D and E. Model number 4 built without ethanol resulted in several negative values, that were all set to zero before calculating points in the Clarke Error Grid. Negative values enable the use of an alarm and are therefore less serious than over-estimating the glucose value, which would instead lead to wrongful insulin administration.

Models 5 and 6 built without APAP and caffeine, respectively, performed similar to some of the random subsets. Although model number 5 has 14.2% of the predicted glucose values in zone B, the inaccuracy is similar to some of the random subset models and can be attributed to inaccuracies in the measurements and not the APAP concentration.

3.3 | Noise characterization and sources of error

There was a drift in temperature as the beam heated the sample. The temperature was measured between 35.6°C and 38.6°C in the course of the experiment, and was seen to drift around 1°C to 2°C in the course of a sample acquisition.

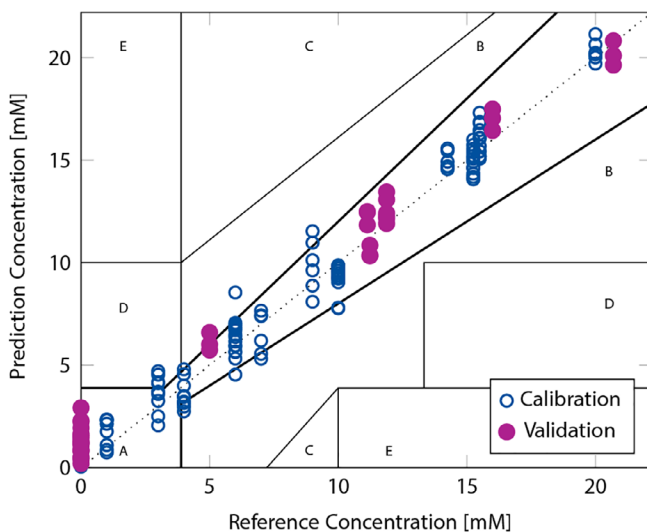


FIGURE 5 Clarke's error grid with calibration on the full set, 97.5% of the validation set was within zone A and the respective 2.5% in zone B

TABLE 2 The ratio of points in the validation set placed in the respective zones of the Clarke's error grid for the models created based on the different sets

Model number	A	B	C	D	E
1. Full	97.5%	2.5%	—	—	—
2. Rand. sub.	88.0%	9.1%	—	2.8%	—
3. No lactate	44.4%	48.1%	—	7.4%	—
4. No ethanol	38.3%	18.5%	—	32.1%	11.1%
5. No APAP	85.2%	14.2%	—	—	—
6. No caffeine	91.4%	7.4%	—	1.2%	—

Abbreviation: APAP, acetaminophen.

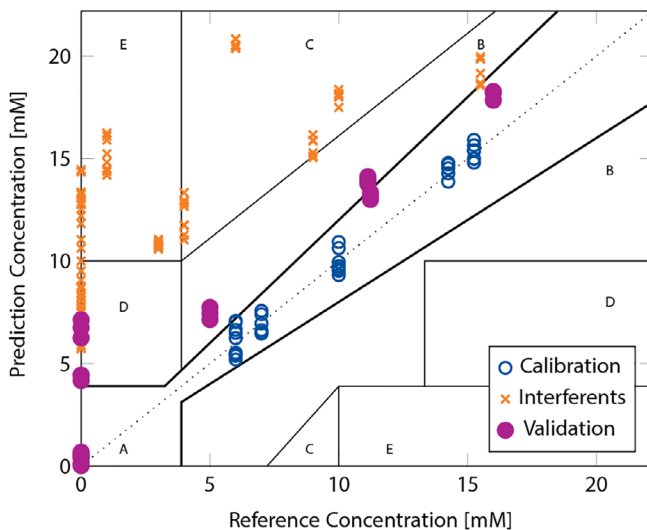


FIGURE 6 Clarke's error grid with calibration on 73 spectra of the set not containing lactate. 44.4% of the validation set was within zone A, 48.1% in zone B and 7.4% in zone D

The spectra were highly temperature dependent, and the difference in temperature is a source of additional variation. Temperature variations could be somewhat compensated by data processing or direct temperature measurement to achieve an improved prediction result [39, 40]. However, as the main objective of this paper was to investigate the effects of interferents, we chose not to introduce other preprocessing and analysis methods that could convolute the molecular interference and temperature effects. For noise analysis, the 100% transmission lines were calculated for water samples obtained throughout the experiment. They were heavily influenced by changes in temperature. The spectrometer specifications state that the photometric noise on the detectors should be $<50 \mu\text{AU}$ for the visible part ($<700 \text{ nm}$) of the spectra, and $<20 \mu\text{AU}$ for the NIR ($>700 \text{ nm}$). The rms noise from the 100% lines was $29 \mu\text{AU}$ for the visible range included in the analysis (500–750 nm), $33 \mu\text{AU}$ for the short wave band (750–1090 nm), $110 \mu\text{AU}$ for the first overtone (1500–1800 nm) and $80 \mu\text{AU}$ for the combination band (2100–2300 nm). Other studies with higher accuracy [41] have presented much lower rms noise, below $10 \mu\text{AU}$. The much higher rms noise of the first overtone can be attributed partly to increased temperature dependence due to water absorption. Water absorption could account for some of the elevated noise for the short wave band and the combination band, but there could also be other sources of noise, for example the temperature change in the air from the air conditioning system [42]. The two downweighted water peaks (at 1800–2100 nm and $>2300 \text{ nm}$) had rms noise around 3 mAU , several orders of magnitudes larger, which confirms the importance of discarding these wavelength channels. A lower noise floor could have improved the accuracy of the predictions in this study, and could have been achieved by

better temperature control (i.e. cooling). In a clinical setting, the temperature is likely to be more stable if the measurement site is within the body, but large variation could be expected if the measurement is performed non-invasively on the skin or minimally invasively in the interstitial fluid. Temperature compensation should then be considered.

Although the noise floor and therefore the RMSEP found in this study is somewhat higher than what has been obtained in other studies with NIR spectroscopy (RMSEPs less than 1 mM) [3, 32, 41], what we learn should also be true for a more accurate model with a lower noise floor, as the absorption is linear. The effect of lactate and ethanol on the predictions are not likely to be improved much with lower noise, as we would not expect finer spectral features that could differentiate the different analytes to emerge in this wavelength range. A higher sensitivity could have revealed very low interference from APAP and caffeine, but we should have seen some systematic error trend if this were the case, which is not present. For CGMs, the elevation in predicted glucose levels due to APAP was 3 to 4 mM [29]. The models presented here would have detected such a degree of interference. As mentioned, APAP and caffeine were not expected to interfere due to the comparably low concentrations they can be found at. We wanted to confirm this due to the great clinical relevance of especially APAP, which interferes with common CGM devices.

As is shown by the Clarke Error Grids, some uncertainty is acceptable, and we could expect future NIR-based glucose measurement devices to have a comparable accuracy as the full model presented due to the generally low SNR, the presence of water, and challenges of implementation in an in vivo setting.

A broad wavelength range was investigated in this preliminary study. When the specific interferents are known, wavelengths with glucose features that are not affected by the interferents can be chosen. The goal in this paper was to investigate which molecules could be interfering, and we therefore conducted a broad wavelength investigation, including some of the visible spectrum. Wavelengths where glucose does not absorb much can also contain glucose information in that the solute (water) spectrum is altered. Including many wavelengths in the NIR can be beneficial because the features are broad and neighboring wavelengths are correlated. By doing a broad scan we can be less sensitive to noise.

3.4 | Verification using biological samples

The full model built with 38 samples used five LVs and had a RMSECV of 44.7 mM, similar to previous studies using this fiber-optic setup [35]. An increase in error with increasing lactate concentrations was not found when lactate was included

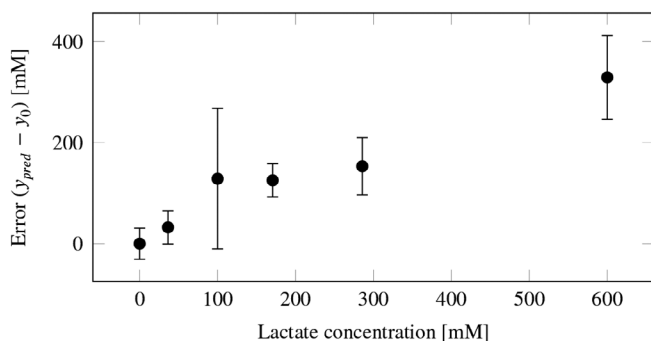


FIGURE 7 The absolute error ($y_{pred} - y_0$) of the glucose model built on samples from porcine intraperitoneal fluid spiked with glucose applied to the same samples spiked with lactate. The error points are grouped in bins for easier readability

in the model. The sub-model built without lactate on 18 samples with three LVs had a RMSECV of 46.3 mM. When this model was applied to the measurements taken on samples with lactate, an increase in error was seen with increasing lactate levels, shown in Figure 7. The dose response was found to be 0.56 mM/mM (95% confidence interval [0.49, 0.63] mM). Although this is slightly higher than the dose response found in the study, the general trend is confirmed.

4 | CONCLUSIONS

Lactate and ethanol at physiological levels were found to interfere with the NIR based glucose prediction when not part of the calibration set. A multivariate model was able to predict the glucose concentration in the presence of the interferents, if they were included in the analysis. The results were verified using peritoneal fluid samples. These results are of medical interest, as a NIR calibration model could be expected to be built on physiological samples, where high levels of lactate and ethanol might not occur. Naturally higher lactate levels can be found during illness and exercise, situations where accurate glucose measurements are important to DM1 patients. Although patients might be asked to exercise before giving samples for a calibration model, patients are not likely to ingest ethanol before delivering such samples. In addition, the use of ethanol affects the glucose levels and can be followed by hypoglycemia [26, 27]. Considering that the user may be intoxicated and be less alert to strange behaviors in their glucose measurement device, it is of paramount importance that prospective NIR-based sensors also calibrate for physiological levels of ethanol.

APAP and caffeine did not appear to affect the predictions of glucose concentrations at the levels measured, as expected. This reveals an advantage of NIR sensing, as APAP is a known interferent to the enzymatic glucose sensors.

To summarize, we have shown how the presence of lactate and ethanol can deteriorate the predictive ability and robustness of the glucose model. With known interferents, it is possible to correct for this in the calibration design and/or chemometric model building. Thus, when the technology is mature enough to go from in vitro to in vivo NIR glucose measurements, lactate and ethanol should be part of the calibration models.

ACKNOWLEDGMENTS

We kindly thank Bjorg Narum from Nofima (Norway) for help and facilitation in acquiring the dataset, and Harald Martens (Idletechs and Department of Cybernetics, NTNU) for his help in data analysis. We also thank Ine Jernelv for her assistance in mixing the validation set, and for access to the initial analysis software [33], and Marte Kierulf Åm and Patrick Bösch for providing the porcine intraperitoneal samples.

Silje S. Fuglerud is funded by the Central Norway Regional Health Authority, project number 46055510. The project is part of the Double Intraperitoneal Artificial Pancreas project, project number 248872, funded by the Research Council of Norway.

CONFLICT OF INTEREST

The authors declare no potential conflict of interests.

AUTHOR CONTRIBUTIONS

Astrid Aksnes: Conceptualization (supporting); funding acquisition (supporting); review and editing (equal). Reinold Ellingsen: Conceptualization (supporting); review and editing (equal). Silje S. Fuglerud: Conceptualization (lead); investigation (lead); formal analysis (lead); writing – original draft (lead); writing – review and editing (equal). Dag R. Hjelme: Conceptualization (supporting); formal analysis (supporting); funding acquisition (lead); writing – review and editing (equal).

DATA AVAILABILITY STATEMENT

The data that support the findings of this study will be openly available in DataverseNO at <http://doi.org/10.18710/NSHFAK>, reference number 37. <https://dataverse.no/privateurl.xhtml?token=1c9e11d0-772d-4012-ba4a-f1892d2d37d6>

ETHICS STATEMENT

The animal experiments in which the intraperitoneal fluid samples were collected were approved by the Norwegian Food Safety Authority (FOTS number 12948) and were in accordance with «The Norwegian Regulation on Animal Experimentation» and «Directive 2010/63/EU on the protection of animals used for scientific purpose».

ORCID

Silje Skeide Fuglerud  <https://orcid.org/0000-0003-2674-6874>

REFERENCES

- [1] Z. Tang, X. Du, R. F. Louie, G. J. Kost, *Am. J. Clin. Pathol.* **2000**, *113*(1), 75. <https://doi.org/10.1309/QAW1-X5XW-BVRQ-5LKQ>.
- [2] A. Basu, M. Q. Slama, W. T. Nicholson, L. Langman, T. Peyser, R. Carter, R. Basu, *J. Diabetes Sci. Technol.* **2017**, *11*(5), 936.
- [3] I. L. Jernelv, K. Milenko, S. S. Fuglerud, D. R. Hjelme, R. Ellingsen, A. Aksnes, *Appl. Spectrosc. Rev.* **2019**, *54*(7), 543. <https://doi.org/10.1080/05704928.2018.1486324>.
- [4] S. F. Malin, T. L. Ruchti, T. B. Blank, S. N. Thennadil, S. L. Monfre, *Clin. Chem.* **1999**, *45*(9), 1651. <https://doi.org/10.1093/clinchem/45.9.1651>.
- [5] D. Barolet, Light-emitting diodes (LEDs) in dermatology. in *Frontline Medical Communications*. Elsevier, Amsterdam, **2008**, p. 227.
- [6] M. Shokrehodaie, S. Quinones, *Sensors* **2020**, *20*(5), 1251.
- [7] D. R. Burnett, L. M. Huyett, H. Zisser, F. Doyle, B. Mensh, *Diabetes* **2014**, *63*, 2498.
- [8] A. L. Fougner, K. Kölle, N. K. Skjærvold, et al., *Model. Identif. Control* **2016**, *37*(2), 121.
- [9] M. K. Åm, A. Fougner, R. Ellingsen, et al., *Med. Hypotheses* **2019**, *132*, 109318.
- [10] G. W. Small, *Trends Anal. Chem.* **2006**, *25*(11), 1057.
- [11] M. A. Arnold, G. W. Small, D. Xiang, J. Qui, D. W. Murhammer, *Anal. Chem.* **2004**, *76*(9), 2583.
- [12] D. Abookasis, J. J. Workman, *J. Biomed. Opt.* **2011**, *16*(2), 027001.
- [13] S. Sharma, M. Goodarzi, L. Wynants, H. Ramon, W. Saeys, *Analytica Chimica Acta* **2013**, *778*, 15. <https://doi.org/10.1016/j.aca.2013.03.045>.
- [14] H. Chung, M. A. Arnold, M. Rhiel, D. W. Murhammer, *Appl. Spectrosc.* **1996**, *50*(2), 270. <https://doi.org/10.1366/0003702963906447>.
- [15] K. H. Hazen, M. A. Arnold, G. W. Small, *Anal. Chim. Acta* **1998**, *371*(2–3), 255. [https://doi.org/10.1016/S0003-2670\(98\)00318-3](https://doi.org/10.1016/S0003-2670(98)00318-3).
- [16] H. Heise, R. Marbach, A. Bittner, T. Koschinsky, *J. Near Infrared Spectrosc.* **1998**, *6*(1), 361.
- [17] T. Yano, T. Funatsu, S. Ki, Y. Nakano, *J. Near Infrared Spectrosc.* **2001**, *9*(1), 43.
- [18] S. Kasemsumran, M. K. Du Yp, M. Huehne, Y. Ozaki, *Analyst* **2003**, *128*(12), 1471.
- [19] J. Chen, M. A. Arnold, G. W. Small, *Anal. Chem.* **2004**, *76*(18), 5405.
- [20] N. Kang, S. Kasemsumran, Y. A. Woo, H. J. Kim, Y. Ozaki, *Chemom. Intell. Lab. Syst.* **2006**, *82*(1), 90–. Selected Papers from the International Conference on Chemometrics and Bioinformatics in Asia. <https://doi.org/10.1016/j.chemolab.2005.08.015>.
- [21] M. Ren, M. A. Arnold, *Anal. Bioanal. Chem.* **2007**, *387*(3), 879.
- [22] R. Henn, C. G. Kirchler, Z. L. Schirmeister, A. Roth, W. Mantele, C. W. Huck, *J. Biophotonics* **2018**, *11*(7), e201700365. <https://doi.org/10.1002/jbio.201700365>.
- [23] Y. Jung, J. Hwang, *Appl. Spectrosc.* **2013**, *67*(2), 171.
- [24] S. Sharma, M. Goodarzi, J. Delanghe, H. Ramon, W. Saeys, *Appl. Spectrosc.* **2014**, *68*(4), 398. <https://doi.org/10.1366/13-07217>.
- [25] Stanley WC, Wisneski JA, Gertz EW, Neese RA, Brooks GA. *Metabolism* **1988**; *37*(9): 850–858. doi: [https://doi.org/10.1016/0026-0495\(88\)90119-9](https://doi.org/10.1016/0026-0495(88)90119-9)
- [26] T. Richardson, M. Weiss, P. Thomas, D. Kerr, *Diabetes Care* **2005**, *28*(7), 1801. <https://doi.org/10.2337/diacare.28.7.1801>.
- [27] P. A. Engler, S. E. Ramsey, R. J. Smith, *Acta Diabetol.* **2013**, *50*(2), 93. <https://doi.org/10.1007/s00592-010-0200-x>.
- [28] L. Dewar, R. Heuberger, *Diabetes Metab. Syndrome Clin. Res. Rev.* **2017**, *11*, S631. <https://doi.org/10.1016/j.dsx.2017.04.017>.
- [29] D. M. Maahs, D. DeSalvo, L. Pyle, T. Ly, L. Messer, P. Clinton, E. Westfall, R. P. Wadwa, B. Buckingham, *Diabetes Care* **2015**, *38*(10), e158. <https://doi.org/10.2337/dc15-1096>.
- [30] P. Calhoun, T. K. Johnson, J. Hughes, D. Price, A. K. Balo, *J. Diabetes Sci. Technol.* **2018**, *12*(2), 393.
- [31] R. W. Bondi, B. Igne, J. K. Drennen, C. A. Anderson, *Appl. Spectrosc.* **2012**, *66*(12), 1442.
- [32] M. Goodarzi, S. Sharma, H. Ramon, W. Saeys, *Trends Anal. Chem.* **2015**, *67*, 147. <https://doi.org/10.1016/j.trac.2014.12.005>.
- [33] I. L. Jernelv, K. Strøm, D. R. Hjelme, A. Aksnes, Mid-infrared spectroscopy with a fiber-coupled tuneable quantum cascade laser for glucose sensing. in *Optical Fibers and Sensors for Medical Diagnostics and Treatment Applications XX. 11233*, 2nd ed. (Ed: I. Gannot), International Society for Optics and Photonics. SPIE, Bellingham, Washington, **2020**, p. 105.
- [34] M. Goodarzi, W. Saeys, *Talanta* **2016**, *146*, 155. <https://doi.org/10.1016/j.talanta.2015.08.033>.
- [35] S. S. Fuglerud, K. B. Milenko, R. Ellingsen, A. Aksnes, D. R. Hjelme, *Appl. Spectrosc.* **2019**, *58*(10), 2456.
- [36] M. K. Åm, K. Kölle, A. L. Fougner, et al., *PLoS One* **2018**, *13*(10). <https://doi.org/10.1371/journal.pone.020>
- [37] M. K. Åm, I. Dirnena-Fusini, A. L. Fougner, S. M. Carlsen, S. C. Christiansen, *Sci. Rep.* **2020**, *10*, 13735.
- [38] W. L. Clarke, D. Cox, L. A. Gonder-Frederick, W. Carter, S. L. Pohl, *Diabetes Care* **1987**, *10*(5), 622. <https://doi.org/10.2337/diacare.10.5.622>.
- [39] K. H. Hazen, M. A. Arnold, G. W. Small, *Appl. Spectrosc.* **1994**, *48*(4), 477. <https://doi.org/10.1366/000370294775268910>.
- [40] H. Martens, S. W. Bruun, I. Adt, G. D. Sockalingum, A. Kohler, *J. Chemometr.* **2006**, *20*(8–10), 402. <https://doi.org/10.1002/cem.1015>.
- [41] K. H. Hazen, M. A. Arnold, G. W. Small, *Appl. Spectrosc.* **1998**, *52*(12), 1597.
- [42] T. Davies, *Spectrosc. Eur.* **2011**, *23*(2), 24.

SUPPORTING INFORMATION

Additional supporting information may be found online in the Supporting Information section at the end of this article.

How to cite this article: Fuglerud SS, Ellingsen R, Aksnes A, Hjelme DR. Investigation of the effect of clinically relevant interferents on glucose monitoring using near-infrared spectroscopy. *J. Biophotonics*. 2021;e202000450. <https://doi.org/10.1002/jbio.202000450>